

Dinuclear Co(II)Co(III) Mixed-Valence and Co(III)Co(III) Complexes with N- and O-Donor Ligands: Characterization and Water Oxidation Studies

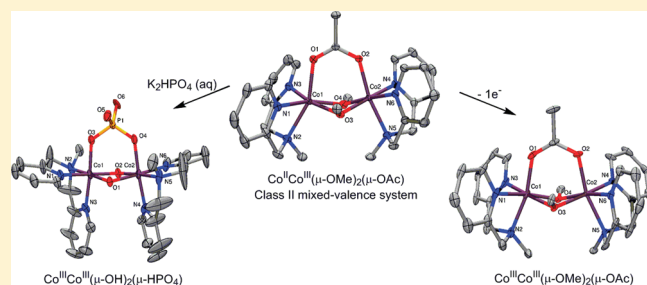
Jia Luo,[†] Nigam P. Rath,[‡] and Liviu M. Mirica^{*,†}

[†]Department of Chemistry, Washington University, One Brookings Drive, St. Louis, Missouri 63130

[‡]Department of Chemistry and Biochemistry, University of Missouri—St. Louis, One University Boulevard, St. Louis, Missouri 63121

S Supporting Information

ABSTRACT: The tridentate ligand *N*-methyl-*N,N*-bis(2-pyridylmethyl)amine (L) has been employed to synthesize a dinuclear Co(II)Co(III) mixed-valence complex containing μ -methoxo and μ -carboxylato bridging ligands, $[\text{LCo}^{\text{II}}(\mu\text{-carboxylato})\text{bis}(\mu\text{-methoxo})\text{Co}^{\text{III}}\text{L}](\text{ClO}_4)_2$. In this complex, the two pseudo-octahedral Co centers have an identical ligand environment, yet the average Co–N and Co–O bond distances at the two Co ions differ significantly. Electrochemical, spectroscopic, and magnetic susceptibility measurements confirm that it belongs to a localized Class II mixed-valence system, despite the presence of a short Co···Co distance of 3.021 Å. Oxidation of this Co(II)Co(III) complex leads to formation of the corresponding Co(III)Co(III) complex that was characterized structurally and spectroscopically. In addition, dinuclear and trinuclear μ -hydroxo Co(III) complexes have been obtained in the presence of phosphate anions and absence of methanol, respectively, suggesting that an additional bridging ligand is needed to stabilize the $\text{Co}^{\text{III}}\text{bis}(\mu\text{-hydroxo})\text{Co}^{\text{III}}$ fragment. Moreover, the ability of the mixed-valence Co(II)Co(III) complex and the three related Co(III) complexes to electrocatalytically oxidize water was also investigated. The observed limited water oxidation catalytic ability for these systems suggests that a multinuclear Co cluster and/or presence of O-rich ligands may be needed for the generation of efficient molecular Co-based water oxidation catalysts.



INTRODUCTION

Since the first synthesis of Prussian blue in 1704, mixed-valence complexes have received considerable attention due to their valence localization/delocalization character and intervalence electronic transitions that can be exploited in magnetism and electrochromism applications.^{1,2} Among dinuclear mixed-valence complexes, Co(II)Co(III) species were rarely reported,^{3–5} and only two other systems contain an octahedral high-spin Co(II) center.^{3a,4} Described herein is the synthesis and characterization of a novel Class II mixed-valence Co(II)Co(III) complex stabilized by a tridentate mononucleating ligand and that contains carboxylate and two methoxide bridging ligands. This system is the first magnetically characterized Co(II)Co(III) mixed-valence complex where both Co centers have an identical ligand environment.^{3a} In addition, three related dinuclear and trinuclear Co(III) complexes have been synthesized and structurally characterized. Moreover, in light of the heterogeneous Co-based water oxidation catalyst reported recently by Nocera et al.,^{6,7} we also investigated the water oxidation ability of the Co(II)Co(III) complex and the three related Co(III) systems. These studies show a limited water oxidation catalytic ability for our complexes, suggesting that a multinuclear Co cluster and/or the presence of O-rich ligands may be needed for generation of efficient molecular Co-based water oxidation catalysts.

EXPERIMENTAL SECTION

Ligand and Complex Syntheses: *N*-Methyl-*N,N*-bis(2-pyridylmethyl)amine, L. L was synthesized following a slightly modified reported procedure.⁸ Formic acid (98%, 11.7 g, 0.25 mol, Fisher Scientific) and formaldehyde (37% aqueous solution, 18.7 mL, 0.25 mol, Aldrich) were mixed thoroughly, and then bis-(2-pyridylmethyl)amine (4.5 mL, 0.025 mol, TCI) was added dropwise. The mixture was heated to reflux for 12 h, cooled to room temperature, and made basic with 3 M NaOH. The product was extracted with anhydrous diethyl ether (4 × 50 mL), the organic layer dried with anhydrous K₂CO₃, and the solvent removed by rotary evaporation. The yellow oil product was purified by vacuum distillation (bp 110 °C, 20 mT) to give a light-yellow oil that was stored at +4 °C. Yield: 4.7 g, 88%. ¹H NMR (CDCl₃, 300 MHz): δ 8.51 (2H, d, pyridine 6-H), 7.7–7.0 (6H, m, pyridine 3, 4, 5-H), 3.73 (4H, s, NCH₂), 2.28 (3H, s, NMe).

[LCo^{II}(μ -O₂CMe)(μ -OMe)₂Co^{III}L](ClO₄)₂, 1. To a stirred solution of L (0.213 g, 0.999 mmol) in MeOH (5 mL), a solution of Co(CO₂Me)₂·4H₂O (0.250 g, 1.00 mmol) in MeOH (5 mL) was added dropwise. The solution was stirred for 10 min, after which H₂O₂ (50 wt %, 28.8 μ L, 0.500 mmol) was added dropwise. After 30 min, 1 equiv of NaClO₄·H₂O (0.145 g, 1.04 mmol) was added and the solution was covered and stirred for an additional 2 h; a brown powder started

Received: February 22, 2011

Published: June 03, 2011

forming after 1 h. The resulting suspension was stored at +4 °C overnight to yield a brown microcrystalline solid that was collected by vacuum filtration and washed with anhydrous diethyl ether. Yield: 0.174 g, 40%. The product was recrystallized from acetonitrile/diethyl ether. Anal. Calcd for $C_{30}H_{39}N_6O_{12}Cl_2Co_2$: C, 41.68; H, 4.55; N, 9.72. Found: C, 41.24; H, 4.55; N, 9.63. UV–vis spectrum [λ_{max} nm (ϵ , $M^{-1} cm^{-1}$), MeCN]: 1071 (10), 569 (100), 426 (620), 373 (290), 264 (12 200). IR (thin film, cm^{-1}): $\nu(\text{MeCO}_2)_{as}$ 1585, $\nu(\text{MeCO}_2)_s$ 1484. ESI-MS (m/z): 332.5843, calcd for $[\text{LCo}^{\text{II}}(\mu\text{-CO}_2\text{Me})(\mu\text{-OMe})_2\text{Co}^{\text{III}}\text{L}]^{2+}$ 332.5843; 764.1188, calcd for $[\text{LCo}^{\text{II}}(\mu\text{-CO}_2\text{Me})(\mu\text{-OMe})_2\text{Co}^{\text{III}}\text{L}](\text{ClO}_4)^+$ 764.1182. Complex **1** shows no EPR signal at 77 K, while at 7 K two broad features are observed at $g \approx 4$ and 2.

$[\text{LCo}^{\text{III}}(\mu\text{-O}_2\text{CMe})(\mu\text{-OMe})_2\text{Co}^{\text{III}}\text{L}](\text{ClO}_4)_3$, **2**. Complex **2** was synthesized by controlled potential electrolysis of **1** (85.1 mg, 98.4 μmol) performed at 1.140 V (vs Ag/0.01 M $\text{AgNO}_3/\text{MeCN}$) using two platinum mesh electrodes as both the working and the auxiliary electrodes, respectively, and Ag/0.01 M $\text{AgNO}_3/\text{MeCN}$ as the reference electrode. The electrolysis was stopped when the charge corresponding to a one-electron oxidation was passed. A dark green solution formed that gave a green powder upon diethyl ether vapor diffusion at -20 °C. The product recrystallized from acetonitrile/diethyl ether. The crystals were collected by vacuum filtration and washed with ether. Yield: 38.2 mg, 40%. Anal. Calcd for $C_{30}H_{39}N_6O_{16}Cl_3Co_2 \cdot 0.5\text{SCH}_3\text{CN}$: C, 37.82; H, 4.15; N, 9.25. Found: C, 37.63; H, 3.95; N, 9.34. UV–vis spectrum [λ_{max} nm (ϵ , $M^{-1} cm^{-1}$), MeCN]: 589 (260), 350 (5,100), 252 (30,700). IR (thin film, cm^{-1}): $\nu(\text{MeCO}_2)_{as}$ 1551, $\nu(\text{MeCO}_2)_s$ 1480. ESI-MS (m/z): 221.7230, calcd for $[\text{LCo}^{\text{III}}(\mu\text{-CO}_2\text{Me})(\mu\text{-OMe})_2\text{Co}^{\text{III}}\text{L}]^{2+}$ 221.7232; 382.0592, calcd for $[\text{LCo}^{\text{III}}(\mu\text{-CO}_2\text{Me})(\mu\text{-OMe})_2\text{Co}^{\text{III}}\text{L}](\text{ClO}_4)^{2+}$ 382.0591; 863.0670, calcd for $[\text{LCo}^{\text{III}}(\mu\text{-CO}_2\text{Me})(\mu\text{-OMe})_2\text{Co}^{\text{III}}\text{L}](\text{ClO}_4)_2^+$ 863.0667.

$[\text{LCo}^{\text{III}}(\mu\text{-PO}_4\text{H})(\mu\text{-OH})_2\text{Co}^{\text{III}}\text{L}](\text{ClO}_4)_2$, **3**. Equimolar amounts of ligand L (0.1066 g, 0.50 mmol) and $\text{Co}(\text{ClO}_4)_2 \cdot 6\text{H}_2\text{O}$ (0.1830 g, 0.50 mmol) were dissolved in 5 mL of MeOH:H₂O (3:1, v:v) separately, and the Co(II) solution was added to the ligand solution dropwise. Then 0.5 equiv of K_2HPO_4 (43.5 mg, 0.25 mmol) was dissolved in a minimum amount of water and slowly added to the reaction mixture while air was bubbled into the solution for 15 min, followed by stirring for 2 h. The initially formed cobalt phosphate purple precipitate was filtered, and the filtrate was layered with diethyl ether. Red crystals formed after 1–2 days. Yield: 31.8 mg, 15%. The low yield of **3** is due to the initial precipitation of the cobalt phosphate side product. Anal. Calcd for $C_{26}H_{33}N_6O_{14}Cl_2Co_2P \cdot 0.5\text{H}_2\text{O} \cdot \text{KClO}_4$: C, 30.59; H, 3.36; N, 8.23. Found: C, 30.91; H, 3.30; N, 8.42. UV–vis spectrum [λ_{max} nm (ϵ , $M^{-1} cm^{-1}$), H₂O]: 530 (130), 373 (sh, 1100), 309 (sh, 6300). IR (film, cm^{-1}): $\nu(\text{OH})$ 3400, $\nu(\text{PO}_4)$ 552, 518. ESI-MS (m/z): 337.0425, calcd for $[\text{LCo}^{\text{III}}(\mu\text{-PO}_4\text{H})(\mu\text{-OH})_2\text{Co}^{\text{III}}\text{L}]^{2+}$ 337.0431; 755.0247, calcd for $[\text{LCo}^{\text{III}}(\mu\text{-PO}_4)(\mu\text{-OH})\text{-Co}^{\text{III}}\text{L}](\text{ClO}_4)^+$ 755.0243; 773.0358, calcd for $[\text{LCo}^{\text{III}}(\mu\text{-PO}_4\text{H})(\mu\text{-OH})_2\text{-Co}^{\text{III}}\text{L}](\text{ClO}_4)^+$ 773.0348.

$[\text{L}_3\text{Co}^{\text{III}}_3(\mu\text{-OH})_4(\text{OH})](\text{ClO}_4)_4$, **4**. Equimolar amounts of ligand L (0.1066 g, 0.50 mmol) and $\text{Co}(\text{CO}_2\text{Me})_2 \cdot 4\text{H}_2\text{O}$ (0.1245 g, 0.50 mmol) were dissolved in 5 mL of acetone:H₂O (3:4, v:v) separately, and the Co(II) solution was added dropwise to the ligand solution, followed by addition of 0.5 equiv of H₂O₂ (50 wt %, 14.4 μL , 0.25 mmol). After 15 min, 3 equiv of $\text{NaClO}_4 \cdot \text{H}_2\text{O}$ (0.2101 g, 1.50 mmol) was added. The solution was stirred for 2 h and layered with diethyl ether to yield red crystals overnight. Yield: 122.5 mg, 56%. Anal. Calcd for $C_{39}H_{50}N_9O_{21}Cl_4Co_3 \cdot \text{CH}_3\text{COCH}_3$: C, 37.16; H, 4.16; N, 9.29. Found: C, 37.26; H, 3.80; N, 9.24. UV–vis spectrum [λ_{max} nm (ϵ , $M^{-1} cm^{-1}$), H₂O]: 519 (240), 314 (5600). IR (film, cm^{-1}): $\nu(\text{OH})$ 3400, $\nu(\text{ClO}_4)$ 1095. ESI-MS (m/z): 675.0587, calcd for $[\text{LCo}^{\text{III}}(\mu\text{-O})_2\text{Co}^{\text{III}}\text{L}](\text{ClO}_4)^+$ 675.0579. The synthesized trinuclear complex has likely dissociated into the dinuclear species, as observed by ESI-MS.

X-ray Diffraction Studies. X-ray diffraction quality crystals of **1** and **2** were obtained by anhydrous diethyl ether vapor diffusion into

acetonitrile solutions. For **3** and **4**, crystals were obtained by layering the solutions with anhydrous diethyl ether. Preliminary examination and data collection were performed using a Bruker Kappa Apex-II Charge Coupled Device (CCD) Detector system single-crystal X-ray diffractometer equipped with an Oxford Cryostream LT device. Data were collected using graphite-monochromated Mo K α radiation ($\lambda = 0.71073$ Å) from a fine focus sealed tube X-ray source. Apex II and SAINT software packages (Bruker Analytical X-ray, Madison, WI, 2008) were used for data collection and data integration. Final cell constants were determined by global refinement of reflections from the complete data set. Data were corrected for systematic errors using SADABS (Bruker Analytical X-ray, Madison, WI, 2008) based on the Laue symmetry using equivalent reflections. Structure solutions and refinement were carried out using the SHELXTL-PLUS software package (Sheldrick, G. M. Bruker-SHELXTL. *Acta Crystallogr.* **2008**, *A64*, 112–122). The structures were refined with full matrix least-squares refinement by minimizing $\sum w(F_o^2 - F_c^2)^2$. All non-hydrogen atoms were refined anisotropically to convergence. All H atoms were added in the calculated position and refined using appropriate riding models (AFIX m3). All data were collected at 100 K, except complex **1** for which data were collected at both 100 and 300 K. Complete listings of geometrical parameters, positional and isotropic displacement coefficients for hydrogen atoms, and anisotropic displacement coefficients for the non-hydrogen atoms are given in the Supporting Information.

Physical Measurements. ¹H (300.121 MHz) NMR spectra were recorded on a Varian Mercury-300 spectrometer. Chemical shifts are reported in ppm and referenced to residual solvent resonance peaks. IR spectra were measured as thin films or KBr plates on a Perkin-Elmer Spectrum BX FT-IR spectrometer in the 4000–400 cm^{-1} range. UV–vis spectra were recorded on a Varian Cary 50 Bio spectrophotometer. Gaussian fitting was performed using Peak functions–GaussAmp in the Origin 7.0 program. EPR spectra were recorded on a JEOL JES-FA X-band (9.2 GHz) EPR spectrometer in a MeCN glass at 120 K. Elemental analyses were carried out by the Columbia Analytical Services Tucson Laboratory. ESI-MS experiments were performed on a Bruker Maxis QTOF mass spectrometer with an electron spray ionization source (Washington University Mass Spectrometry Resource, a NIH Research Resource, Grant No. P41RR0954). Room-temperature magnetic susceptibility measurements in the solid state were performed using a Faraday balance by the Gouy method.⁹ Solution state magnetic susceptibility at room temperature was obtained by the Evans method in CD₃CN using a 300 MHz NMR spectrometer.¹⁰ Variable-temperature magnetic measurement was performed using a Quantum Design Physical Properties Measurement System, working in the range 4.2–300 K under a magnetic field of 2 T and at 4.2 K from 0 to 9 T (Center of Materials Innovation, Washington University). Susceptibilities were corrected for the diamagnetic contribution by using Pascal's constants.¹¹ Cyclic voltammograms were recorded using a BASi EC Epsilon electrochemical workstation and a glassy carbon working electrode (GCE), a platinum-wire auxiliary electrode, and a Ag/0.01 M $\text{AgNO}_3/\text{MeCN}$ reference electrode. Before every use the working electrode was polished with 0.05 μm alumina particles for 30 s and cleaned with deionized water by ultrasonication for 1 min. Electrochemical-grade $\text{Bu}_4\text{N}^+\text{ClO}_4^-$ (tetrabutylammonium perchlorate, TBAP) from Fluka was used as the supporting electrolyte at a concentration of 0.1 M in nonaqueous solutions. Potentials are reported relative to Fc^+/Fc in TBAP/MeCN; the potential of ferrocene is 87 mV against Ag/0.01 M $\text{AgNO}_3/\text{MeCN}$. In aqueous solutions, the Ag/AgCl electrode (0.197 V vs NHE) was used as the reference and a 0.1 M $\text{KH}_2\text{PO}_4/\text{K}_2\text{HPO}_4$ buffer (KPi, pH 7) was used as the supporting electrolyte. The analyzed solutions were deaerated by purging with nitrogen for 10 min. Controlled potential water oxidation electrolysis was performed using a two-compartment cell with a fine-porosity glass frit junction. A 2 cm \times 1 cm indium tin oxide electrode (ITO, resistivity 8–12 Ω per square inch,

Scheme 1. Synthesis of the Co Complexes

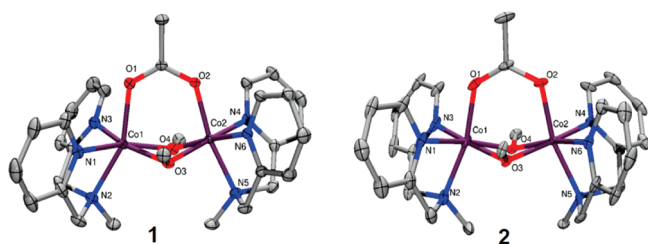
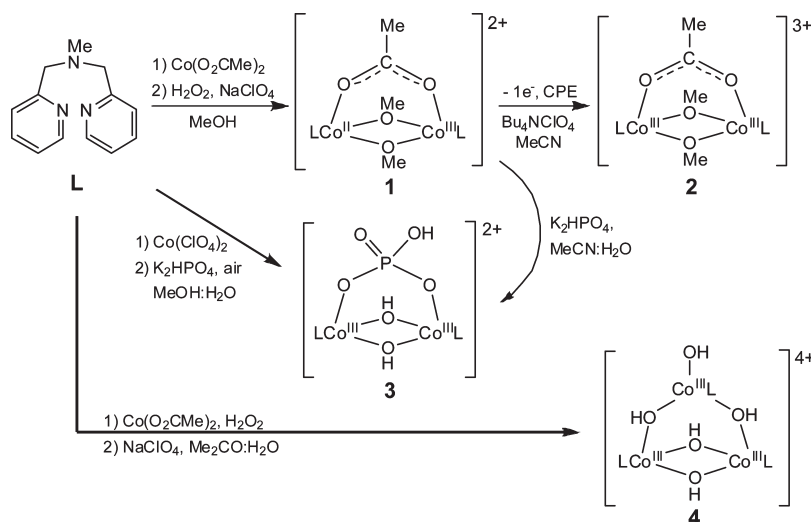


Figure 1. ORTEP diagram for **1** and **2** with 50% thermal ellipsoids (the ClO_4^- counteranions and H atoms were omitted for clarity). Selected bond distances (Å) for **1** $\text{Co1}-\text{O}_{\text{ave}}$ 2.066, $\text{Co1}-\text{N}_{\text{ave}}$ 2.147, $\text{Co2}-\text{O}_{\text{ave}}$ 1.902, $\text{Co2}-\text{N}_{\text{ave}}$ 1.957, $\text{Co1}\cdots\text{Co2}$ 3.021 and for **2** $\text{Co1}-\text{O}_{\text{ave}}$ 1.920, $\text{Co1}-\text{N}_{\text{ave}}$ 1.960, $\text{Co2}-\text{O}_{\text{ave}}$ 1.928, $\text{Co2}-\text{N}_{\text{ave}}$ 1.962, $\text{Co1}\cdots\text{Co2}$ 2.956.

Aldrich) was used as the working electrode, while a platinum mesh and a Ag/AgCl electrode were used as the auxiliary and reference electrodes, respectively, and 0.1 M KPi pH 7 was used as the supporting electrolyte. The area of the ITO inserted into the solution was approximately 1 cm^2 . For water oxidation studies, a solution of **1** or **2** in MeCN or $\text{Co}(\text{ClO}_4)_2$ in H_2O was quantitatively dropped on the ITO with a microsyringe (1.2×10^{-7} mol per cm^2 for complexes and 2.4×10^{-7} mol per cm^2 for $\text{Co}(\text{ClO}_4)_2$).¹² For the water-soluble complexes **3** or **4**, a solution in KPi (0.5 mM) was used directly (when **3** or **4** was deposited on ITO, the measured current was very small, $<15\ \mu\text{A}$). A FOXY O_2 fluorescent probe (Ocean Optics) was employed to detect the amount of O_2 produced during electrolysis.

RESULTS AND DISCUSSION

Synthesis and Structures of Complexes 1–4. Complex **1** was prepared by adding *N*-methyl-*N,N*-bis(2-pyridylmethyl)amine (L) to $\text{Co}(\text{OAc})_2$ in MeOH followed by addition of an equivalent amount of hydrogen peroxide (Scheme 1).^{13,14} Addition of H_2O_2 is required for the formation of the complex. The X-ray structure of **1** reveals a dinuclear mixed-valence $\text{Co}(\text{II})\text{Co}(\text{III})$ complex, $[\text{LCo}^{\text{II}}(\mu\text{-O}_2\text{CMe})(\mu\text{-OMe})_2\text{Co}^{\text{III}}\text{L}](\text{ClO}_4)_2$ (Figure 1). While both Co centers have a pseudo-octahedral geometry, the average Co–N and Co–O bond distances of the Co1 center are 2.15 and 2.07 Å, respectively, longer than the similar bond length

averages of 1.96 and 1.90 Å for the Co2 center. The observed bond length differences of 0.18–0.19 Å for the Co1 vs the Co2 center are typical for high-spin $\text{Co}(\text{II})$ vs low-spin $\text{Co}(\text{III})$ centers,^{3,4} suggesting that **1** can be best described as a localized Class II mixed-valence dinuclear complex.² The X-ray diffraction pattern obtained at 300 K reveals a structure that is identical to that at 100 K, showing that **1** is a mixed-valence system over the entire temperature range.¹⁴ However, the two Co centers have an identical ligand environment, and the $\text{Co}\cdots\text{Co}$ distance of 3.021 Å in **1** is the shortest among all reported mixed-valence $\text{Co}(\text{II})\text{Co}(\text{III})$ complexes,^{3–5} and thus, it prompted us to investigate in detail the electronic properties of this system (vide infra).

Controlled potential electrolysis of **1** at 1.05 V vs Fc^+/Fc in MeCN yielded a green product that formed after the charge equivalent to a one-electron oxidation had passed. X-ray structural characterization of the green complex reveals an almost C_2 -symmetric structure corresponding to $[\text{LCo}^{\text{III}}(\mu\text{-O}_2\text{CMe})(\mu\text{-OMe})_2\text{Co}^{\text{III}}\text{L}](\text{ClO}_4)_3$, **2**. Both Co centers have a pseudo-octahedral geometry and similar metrical parameters with average Co–N and Co–O bond distances of 1.96 and 1.92 Å, respectively, confirming the presence of two $\text{Co}(\text{III})$ centers (Figure 1). The more compact structure of **2** exhibits a $\text{Co}\cdots\text{Co}$ distance of 2.956 Å, which is ~ 0.06 Å shorter than that found for **1**.

When ligand L was reacted in a methanol–water solution with $\text{Co}(\text{ClO}_4)_2 \cdot 6\text{H}_2\text{O}$ instead of $\text{Co}(\text{OAc})_2 \cdot 4\text{H}_2\text{O}$, to avoid the presence of the carboxylate ions, addition of K_2HPO_4 led to formation of the bis(μ -hydroxide), phosphate-bridged dinuclear complex $[\text{LCo}^{\text{III}}(\mu\text{-PO}_4\text{H})(\mu\text{-OH})_2\text{Co}^{\text{III}}\text{L}](\text{ClO}_4)_2$, **3**. The added K_2HPO_4 provides the phosphate-bridging ligand needed to complete the octahedral coordination of each $\text{Co}(\text{III})$ center, while the hydroxide bridging ligands are derived from water (Scheme 1 and Figure 2). The relatively low yield of the reaction is due to the formation of the insoluble cobalt(III) phosphate side product. In addition, the diffraction data for **3** suffers from disorder and twinning; thus, this structure is used only to obtain atom connectivity information.

Interestingly, the use of $\text{Co}(\text{OAc})_2 \cdot 4\text{H}_2\text{O}$ as the metal salt in an acetone–water mixture yielded the trinuclear, hydroxide-bridged complex $[\text{L}_3\text{Co}^{\text{III}}_3(\mu\text{-OH})_4(\text{OH})](\text{ClO}_4)_4$, **4**, where the

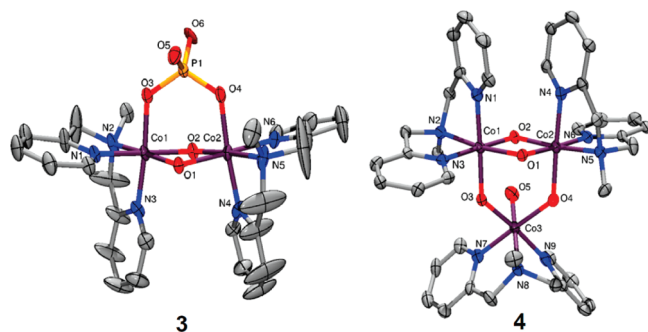


Figure 2. X-ray crystal structures of **3** and **4** (the counteranions and H atoms were omitted for clarity). See Supporting Information for metrical parameters.

Table 1. Electrochemical and UV–Vis Data for Complexes **1–4**^a

	$E_{pa}^{II,III/III,III}, E_{pc}^{III,III/II,III}, E_{pc}^{II,III/II,II}$ (V) ^b	UV–vis, λ , nm (ϵ , M ⁻¹ cm ⁻¹)
1	1.34, 0.65, -0.08 (irrev ^c)	1071 (10), 569 (100), 426 (620), 373 (290), 264 (12,200)
2	1.35, 0.62, -0.08 (irrev)	589 (260), 350 (5,100), 252 (30,700)
3	-0.01 (irrev), -0.30 (irrev)	530 (130), 373 (1,100), 309 (6,300)
4	0.21 (irrev), -0.30 (irrev)	519 (240), 314 (5,600)

^aData were recorded in MeCN for **1** and **2** and in aqueous solutions for **3** and **4**. ^bMeasured by cyclic voltammetry and reported vs NHE (scan rate 100 mV/s). ^cIrreversible.

bridging counteranion has been replaced by a LCo(μ -OH)₂ fragment (Scheme 1 and Figure 2).¹⁴ All three Co centers have metrical parameters suggestive of Co(III) ions: the Co1 and Co2 centers are similar to the Co centers in **2** and **3**, while a terminal hydroxide ligand completes the octahedral geometry of the Co3 ion. While numerous examples exist of trinuclear Co(III) complexes with three μ_2 -hydroxide and one μ_3 -oxo bridging ligands (i.e., a Co₃O₄ core), complex **4** is to the best of our knowledge the first nonlinear trinuclear Co complex that does not have a μ_3 -bridging ligand.¹⁵

Cyclic Voltammetry. The cyclic voltammogram (CV) of **1** in MeCN displays a quasi-reversible oxidation with the anodic wave at 1.34 V vs NHE (0.72 vs Fc⁺/Fc), the cathodic wave at 0.65 V vs NHE (0.03 V vs Fc⁺/Fc), and an irreversible reduction peak at -0.08 V (-0.70 V vs Fc⁺/Fc, Table 1). The reduction peak at 0.65 V was not observed if scanning negatively first, supporting its association with the oxidation wave at 1.34 V, both being assigned to the Co(II)Co(III)/Co(III)Co(III) redox couple (Figure S5, Supporting Information). The ~700 mV peak-to-peak separation of the quasi-reversible oxidation process is indicative of a chemically reversible but electrochemically quasi-reversible process, as expected for the structural reorganization occurring upon oxidation from Co(II) in **1** to Co(III) in **2**. The reduction at -0.08 V, assigned to a Co(II)Co(III) → Co(II)Co(II) process is irreversible most likely due to the lability of the Co(II) centers on the voltammetric time scale. Moreover, no additional oxidation waves have been observed in the cathodic scan up to 2.3 V vs NHE (1.7 V vs Fc⁺/Fc), suggesting that **1** cannot access the Co(IV) oxidation state under electrochemistry conditions. A similar CV was observed for **2** except that the oxidation peak appears only after the initial cathodic scan, confirming that the

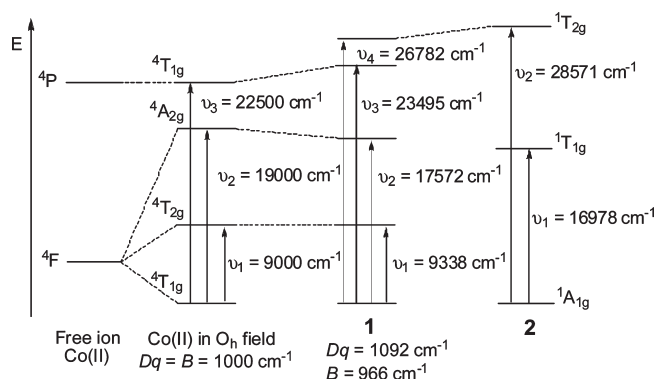


Figure 3. Energy diagram showing the electronic transitions for the Co(II)Co(III) complex **1** and the Co(III)Co(III) complex **2**.

assignment of this oxidation peak is Co(II)Co(III) → Co(III)Co(III).¹⁴

The CV of **3** (0.5 mM) in 0.1 M KPi (pH 7) shows two irreversible reduction peaks at ~-10 and ~-300 mV vs NHE, and no oxidation peak was observed in the first anodic scan (Table 1). In addition, the CV does not change when multiple scans (>10) were carried out within the range of 0.5–1.7 V.¹⁴ Similarly, the CV of **4** in 0.1 M KPi (pH 7) reveals two irreversible reductions at 210 and -300 mV vs NHE. On the basis of the ESI-MS result, **4** can dissociate in solution into a dinuclear Co(III)(μ -OH)₂Co(III) complex that exhibits a CV similar to **3**.¹⁴

UV–Vis Spectroscopy. The absorption spectrum of **1** in MeCN reveals transitions at 1071, 569, 426, and 373 nm (Table 1 and Figures S12 and S13, Supporting Information), while **2** exhibits two absorption bands at 589 and 350 nm. Since **1** contains both Co(II) and Co(III) centers, the band at 373 nm (ν_4 , 26 782 cm⁻¹) is assigned as a d–d transition of the Co(III) center (Figure 3).¹⁶ The other three absorption bands at 1071 (ν_1 , 9338 cm⁻¹), 569 (ν_2 , 17 572 cm⁻¹), and 426 nm (ν_3 , 23 495 cm⁻¹) are assigned to the three spin-allowed transitions expected for a high-spin Co(II) in a pseudo-octahedral geometry: $4T_{1g} \rightarrow 4T_{2g}$, $4T_{1g} \rightarrow 4A_{2g}$, and $4T_{1g}(F) \rightarrow 4T_{1g}(P)$, respectively.¹⁷ The extinction coefficient of the 1071 nm band is ~10 M⁻¹ cm⁻¹, much lower than the usual value of ~1000 M⁻¹ cm⁻¹ for charge transfer bands, further suggesting that **1** is a Class II mixed-valence system.¹⁴ Through Lever's derivation¹⁸ the two ligand field parameters Dq and Racah B were calculated to be 966 and 1092 cm⁻¹, respectively,¹⁴ and the A factor (i.e., the degree of mixing of the two $4T_{1g}$ states arising from the $4F$ and $4P$ terms)¹⁹ was found to be 1.43, suggestive of a weak ligand field for the Co(II) center in **1**.^{4,17,20,21} By comparison, the UV–vis spectrum of **3** in a 0.1 M KPi aqueous solution exhibits absorption bands at 530 and 373 nm, while the spectrum of **4** in 0.1 M KPi shows two bands at 519 and 314 nm (Table 1 and Figure S17, Supporting Information), both spectra being characteristic of Co(III) species.

The stability of **1** and **2** under aqueous conditions was tested by recording their UV–vis spectra in 1:1 (v:v) MeCN: 0.1 M KPi_{aq} pH 7 solution (Figures S15 and S16, Supporting Information). While the UV–vis spectrum of **2** did not change upon addition of the KPi solution, for **1** a new absorbance band at 520 nm and a shoulder at ~370 nm were observed, suggesting that **1** reacts with KPi to generate a new species that has an absorption profile similar to the bis(μ -hydroxide), phosphate-bridged

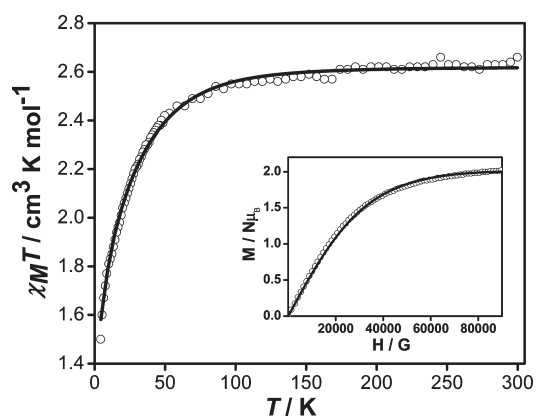


Figure 4. Plot of χ_{MT} vs T for **1**. Experimental data (open circles) and the best fit (black line) using the Hamiltonian described in the text. (Inset) Plot of the reduced magnetization ($M/N\beta$) at 4.2 K for **1** (open circles) and the fit to the Brillouin equation for $S' = 0.5$ and $g = 4.04$ (black line).

dinuclear complex **3** (Figure S15, Supporting Information). This is confirmed by ESI-MS analysis of the solution of **1** in MeCN:0.1 M KPi that reveals one peak at 755.0521 assigned to $[\text{LCo}^{\text{III}}(\mu\text{-OH})(\mu\text{-PO}_4)\text{Co}^{\text{III}}\text{L}](\text{ClO}_4)^+$ (calculated 755.0243), suggesting that a species with HO^- and/or HPO_4^{2-} bridging ligands (i.e., analogous to **3**) has been formed in the presence of aqueous KPi (Scheme 1).

Magnetic Properties of 1. Room-temperature magnetic moment measurements of **1** were performed both in solution and in the solid state to give a value of $\sim 4.2 \mu_{\text{B}}$, typical for a high-spin Co(II) center.⁴ Variable-temperature magnetic susceptibility measurements reveal decreasing χ_{MT} values from $2.61 \text{ cm}^3 \text{ K mol}^{-1}$ at 300 K to $1.51 \text{ cm}^3 \text{ K mol}^{-1}$ at 4.2 K, characteristic of the spin-orbit coupling effects for high-spin octahedral Co(II) ions. The full Hamiltonian describing the magnetic properties of an isolated octahedral Co(II) ion, including the spin-orbit coupling, axial distortion, and Zeeman interaction is given by

$$\hat{H} = -Ak\lambda LS + \Delta[L_z^2 - (1/3)L(L+1)] + \mu_{\text{B}}(-AkL + g_e S)H \quad (1)$$

where the A factor was defined above, κ is the reduction of the orbital momentum caused by the delocalization of the unpaired electrons, λ is the spin-orbit coupling constant, and Δ is an axial distortion factor. As an exact analytical expression to describe the magnetic susceptibility of a Co(II) ion in a distorted octahedral geometry cannot be derived,⁴ an empirical expression developed by Lloret et al. was employed.²¹ By employing this empirical expression, the best fit to the experimental data of **1** gave $\alpha = A\kappa = 1.16$, $\Delta = 498 \text{ cm}^{-1}$, and $\lambda = -89 \text{ cm}^{-1}$ (Figure 4).¹⁴ These values are within the range for high-spin octahedral Co(II) centers.^{4,17,20,21} The α value suggests a weak ligand field with a small orbital reduction factor, while the Δ value confirms the axial distortion as observed in the crystal structure. The slightly lower than normal $|\lambda|$ value may be due to a very small degree of delocalization found in **1**,⁴ likely due to the identical ligand environment of the two Co centers.

The reduced magnetization ($M/N\beta$) for **1** at 4.2 K reaches a saturation M_s value of $2.02 \mu_{\text{B}}$ at 80 kG (Figure 4, inset). This value is smaller than the expected value of 3 for $g = 2$ due to the fact that only the ground state Kramers doublet is populated at

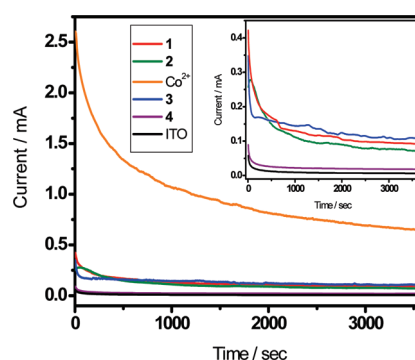


Figure 5. Bulk electrolysis at 1.597 V vs NHE in 0.1 M KPi pH 7. The ITO electrode was coated with **1** or **2** ($1.2 \times 10^{-7} \text{ mol/cm}^2$) or $\text{Co}(\text{ClO}_4)_2$ ($2.4 \times 10^{-7} \text{ mol/cm}^2$). For **3** and **4**, a 0.5 mM solution in 0.1 M KPi was employed. (Inset) Expanded electrolysis traces for **1**, **2**, **3**, and **4**. The current corresponding to the blank ITO electrode control is shown in black.

4.2 K, with an effective spin $S' = 1/2$ with $g = (10 + 2\alpha)/3 = 4.10$ similar to the experimental value of 4.04. Overall, the magnetic behavior of the **1** is in agreement with the presence of an isolated Co(II) ion. Additional evidence for **1** being a localized Class II mixed-valence system is provided by the DFT-calculated spin density showing that less than 0.3% of the total spin density is found on the Co(III) center (Figure S18, Supporting Information).

Water Oxidation Studies. The distinctive electronic properties of the mixed-valence Co(II)Co(III) complex **1** and its potential relevance to the heterogeneous Co-based water oxidation catalyst^{6,7} have prompted us to investigate the water oxidation ability of **1** and **2**. When a small amount of water was added to a 1 mM solution of **1** and **2** in 0.1 M TBAP/MeCN, the CV shows a current increase in the anodic region, likely due to water oxidation, although no distinct oxidation wave was observed (Figure S6, Supporting Information). A similar current increase was also observed for **2**, suggesting that both **1** and **2** may have the ability to catalyze water oxidation. Thus, water electrolysis studies were performed at 1.597 V vs NHE (0.973 V vs Fc^+/Fc) in 0.1 M phosphate buffer (KPi), pH 7. Due to the low solubility of **1** and **2** in H_2O , an indium tin oxide (ITO) electrode coated with $1.2 \times 10^{-7} \text{ mol}$ of either **1** or **2** was used as the working electrode. Both complexes showed a low initial catalytic current ($< 0.5 \text{ mA}$) that dropped rapidly to reach a steady state of $\sim 0.1 \text{ mA}$ after 1 h (Figure 5), during which time a charge of $\sim 0.5 \text{ C}$ passed for both complexes, corresponding to a theoretical amount of $\sim 1.3 \mu\text{mol}$ of O_2 . During electrolysis bubbles formed on the ITO surface coated with **1**, and a value of $2.5 \pm 0.7 \mu\text{mol O}_2$ produced was measured by a fluorescent probe (Figure S19, Supporting Information), yet the value is too small to be precisely measured (no bubbles were observed in a control experiment with a blank ITO electrode).¹⁴ While H_2O_2 could be produced instead of O_2 , the applied electrolysis potential is expected to rapidly oxidize the formed H_2O_2 to O_2 (the $\text{O}_2/\text{H}_2\text{O}_2$ potential is 0.281 V vs NHE at pH 7). No large difference in water oxidation was observed between complexes **1** and **2**, suggesting that the oxidation state of the Co centers is not markedly affecting their reactivity.

A control electrolysis experiment using an ITO electrode coated with $2.4 \times 10^{-7} \text{ mol}$ of $\text{Co}(\text{ClO}_4)_2$ reveals a higher current corresponding to a charge of 3.54 C in 1 h.¹⁴ The final current density of $\sim 0.7 \text{ mA/cm}^2$ is similar to Nocera's system

(~ 1.1 mA/cm²), and a brown coating forms on the ITO surface, suggesting generation of a heterogeneous Co-based water oxidation catalyst in situ.^{6,14}

Since complex **3** is analogous to the species generated by adding aqueous KPi to a MeCN solution of **1** and **4** has a structure resembling the minimal unit that could exist in Nocera's heterogeneous Co–O catalyst (Figure 2),^{6,7} water oxidation studies were also carried out for complexes **3** and **4**. When a potential of 1.597 V vs NHE was applied to 0.5 mM solutions of **3** and **4** in 0.1 M KPi pH 7, a limited water oxidation ability was revealed for **3**, while a lack of water oxidation reactivity was observed for **4** (Figure 5). UV–vis spectra before and after water electrolysis for both solutions of **3** and **4** are unchanged,¹⁴ indicating that these complexes remain intact under these electrolysis conditions. Overall, these results suggest that the investigated dinuclear and trinuclear Co complexes are not efficient water oxidation electrocatalysts.

CONCLUSION

Using the tridentate ligand *N*-methyl-*N,N*-bis(2-pyridylmethyl)amine (L) we synthesized a dinuclear Co(II)Co(III) complex containing μ -methoxy and μ -carboxylato bridging ligands and where both Co centers have a pseudo-octahedral geometry and an identical ligand environment. Structural, electrochemical, spectroscopic, and magnetic studies suggest that this complex is a Class II, localized mixed-valence system. In addition, the corresponding one-electron oxidized Co(III)Co(III) dinuclear complex and two additional Co(III) complexes with μ -hydroxo and μ -phosphato bridging ligands have been structurally characterized. The potential water oxidation catalytic ability of the four Co complexes has been investigated; however, all the synthesized Co complexes are not efficient water oxidation catalysts. The results reported herein suggest that a dinuclear (or trinuclear) Co complex may not be sufficient for the formation of a molecular water oxidation catalyst. Moreover, we suggest that for the investigated Co complexes with N- and O-donor ligands a Co(IV) intermediate²² cannot be accessed and as such these systems should not be able to oxidize water efficiently. Our current research efforts are aimed at investigating whether dinuclear, hydroxide-bridged complexes of other transition metals or employing additional O-rich ligands can act as homogeneous water oxidation catalysts.

ASSOCIATED CONTENT

S Supporting Information. X-ray crystal structure data, electrochemical, spectroscopic, and magnetic characterization, and computational details. This material is available free of charge via the Internet at <http://pubs.acs.org>.

AUTHOR INFORMATION

Corresponding Author

*E-mail: mirica@wustl.edu.

ACKNOWLEDGMENT

This work was generously supported by startup funds from Washington University and an ACS-PRF Doctoral New Investigator grant (49914-DNI3). We thank Prof. Joan Cano for very helpful discussions on the magnetism of **1**.

REFERENCES

- (1) Robin, M. B.; Day, P. *Adv. Inorg. Chem. Radiochem.* **1967**, *10*, 247.
- (2) (a) Taube, H. *Angew. Chem., Int. Ed.* **1984**, *23*, 329. (b) Prassides, K. *Mixed Valency Systems—Applications in Chemistry, Physics and Biology*; Kluwer Academic Publishers: Dordrecht, 1991; (c) Astruc, D. *Acc. Chem. Res.* **1997**, *30*, 383. (d) McCleverty, J. A.; Ward, M. D. *Acc. Chem. Res.* **1998**, *31*, 842. (e) Kaim, W.; Klein, A.; Glockle, M. *Acc. Chem. Res.* **2000**, *33*, 755.
- (3) (a) Chaudhuri, P.; Querbach, J.; Wiegardt, K. *J. Chem. Soc., Dalton Trans.* **1990**, 271. (b) Hemmert, C.; Gornitzka, H.; Meunier, B. *New J. Chem.* **2000**, *24*, 949. (c) Chiari, B.; Cinti, A.; Crispin, O.; Demartin, F.; Pasini, A.; Piovesana, O. *J. Chem. Soc., Dalton Trans.* **2001**, 3611.
- (4) Fondo, M.; Ocampo, N.; Garcia-Deibe, A. M.; Corbella, M.; Fallah, M. S. E.; Cano, J.; Sanmartin, J.; Bermejo, M. R. *Dalton Trans.* **2006**, 4905.
- (5) Szymczak, N. K.; Berben, L. A.; Peters, J. C. *Chem. Commun.* **2009**, 6729.
- (6) Kanan, M. W.; Nocera, D. G. *Science* **2008**, *321*, 1072.
- (7) Kanan, M. W.; Surendranath, Y.; Nocera, D. G. *Chem. Soc. Rev.* **2009**, *38*, 109.
- (8) Jensen, K. B.; McKenzie, C. J.; Simonsen, O.; Tofflund, H.; Hazell, A. *Inorg. Chim. Acta* **1997**, *257*, 163.
- (9) Saunderson, A. *Phys. Educ.* **1968**, *3*, 272.
- (10) Loliger, J.; Scheffold, R. *J. Chem. Educ.* **1972**, *49*, 646.
- (11) Bain, G. A.; Berry, J. F. *J. Chem. Educ.* **2008**, *85*, 532.
- (12) Wada, T.; Tsuge, K.; Tanaka, K. *Angew. Chem., Int. Ed.* **2000**, *39*, 1479.
- (13) Mukherjee, J.; Balamurugan, V.; Gupta, R.; Mukherjee, R. *Dalton Trans.* **2003**, 3686.
- (14) See the Supporting Information.
- (15) Ama, T.; Rashid, M. M.; Yonemura, T.; Kawaguchi, H.; Yasui, T. *Coord. Chem. Rev.* **2000**, *198*, 101.
- (16) Kember, M. R.; White, A. J. P.; Williams, C. K. *Macromolecules* **2010**, *43*, 2291.
- (17) Herrera, J. M.; Bleuzen, A.; Dremzee, Y.; Julve, M.; Lloret, F.; Verdager, M. *Inorg. Chem.* **2003**, *42*, 7052.
- (18) Lever, A. B. P. *J. Chem. Educ.* **1968**, *45*, 711.
- (19) Figgis, B. N.; Gerloch, M.; Lewis, J.; Mabbs, F. E.; Webb, G. A. *J. Chem. Soc.* **1968**, 2086.
- (20) Colacio, E.; Lloret, F.; Ben Maimoun, I.; Kivekas, R.; Sillanpaa, R.; Suarez-Varela, J. *Inorg. Chem.* **2003**, *42*, 2720.
- (21) Lloret, F.; Julve, M.; Cano, J.; Ruiz-Garcia, R.; Pardo, E. *Inorg. Chim. Acta* **2008**, *361*, 3432.
- (22) McAlpin, J. G.; Surendranath, Y.; Dinca, M.; Stich, T. A.; Stoian, S. A.; Casey, W. H.; Nocera, D. G.; Britt, R. D. *J. Am. Chem. Soc.* **2010**, *132*, 6882.